Evaluation of Range-Separated Hybrid and Other Density Functional Approaches on Test Sets Relevant for Transition Metal-Based Homogeneous Catalysts†

Carlos A. Jiménez-Hoyos, Benjamin G. Janesko, and Gustavo E. Scuseria*

Department of Chemistry, Rice University, Houston, Texas 77005

Received: March 30, 2009; Revised Manuscript Received: June 3, 2009

Homogeneous catalysis by transition metal complexes is challenging to model with electronic structure theory. This is due to the large system sizes encountered, the wide range of bonding motifs, and the need for accurate treatments of reaction kinetics. Range-separated hybrid density functionals have been shown to accurately predict a variety of properties in (organic) main group chemistry. Here we benchmark representative range-separated hybrids for geometric and energetic properties of transition metal complexes. Results from conventional semilocal and global hybrid approaches are included for comparison. The range-separated hybrids' performance, combined with their demonstrated accuracy for main group kinetics, makes them promising for applications to homogeneous catalysis. Our results also point to the importance of the correlation functional in range-separated hybrids.

Introduction

Density functional theory (DFT) is one of the most widely used theoretical tools for modeling transition metal compounds. Ground-state DFT has become a standard treatment for geometries and vibrational frequencies[1] of transition metal complexes, reaction barriers in homogeneous transition metal catalysis,[2,3] and the active site in combined QM/MM simulations of metalloenzymes.[4]

DFT's widespread adoption for modeling transition metals is due in part to the limited alternatives. Transition metal complexes are much more challenging than (organic) main group chemistry for high-level ab initio electronic structure calculations.[5] This is a consequence of the wide range of bonding motifs available in transition metals, the relatively large size of many transition metal complexes, and the presence of strong nondynamical correlation effects (as in the archetypal Cr_2 hextuple bond)[6] necessitating expensive multireference treatments. While semiempirical methods can account for some of these effects,[7] standard single-reference Kohn−Sham density functional theory with approximate exchange-correlation functionals often provides the best available trade-off between accuracy and computational expense.

A drawback of most[8] approximate exchange-correlation functionals is that they do not systematically converge to the exact functional. They are usually validated against (and sometimes parametrized to) accurate experimental[9,10] and/or ab initio[11] results. With a few notable exceptions,[12−16] the early years of density functional development focused on validation for (organic) main group chemistry. However, there has been a recent surge of interest among density functional developers in benchmarking to transition metal data.[17] (The work of Furche and Perdew[18] played a particularly important role in this regard.)

The diversity of transition metal chemistry, the difficulty of accurate ab initio calculations, and the paucity of gas-phase experiments makes construction of accurate and comprehensive transition metal benchmark sets a serious challenge. However, several groups have risen to this challenge and assembled test sets for a range of transition metal properties (see Table 1). Bühl and co-workers presented data sets of accurate metal−ligand bond lengths from coordinatively saturated 3d, 4d, and 5d transition metal complexes, obtained from gas-phase electron diffraction and microwave spectroscopic data.[19−22] These authors also report a smaller data set of 3d metal−halide bond lengths, obtained from high-temperature gas-phase electron diffraction experiments.[19] Johnson and Becke[23] recently compiled a set of mean-ligand removal enthalpies for 3d closed-shell transition metal complexes. Furche and Perdew[18] performed an extensive survey of DFT for 3d transition metal chemistry, analyzing accurate reaction energies from a wide range of M−X binding motifs (M = 3d metal, X = M, H, O, N, F, and CO) as well as some coordinatively saturated compounds. Their reference set is somewhat biased toward coordinatively unsaturated compounds, thus approximations that are problematic for this set may still be appropriate for the more restrictive case of coordinatively saturated compounds. Other recently developed transition metal test sets include those of Riley and Merz,[24] Schultz, Zhao, and Truhlar,[25,26] and Hyla-Kryspin and Grimme.[27]

In the present work, we benchmark three of our range-separated hybrid density functionals against the transition metal test sets of Bühl and co-workers, Furche and Perdew, and Johnson and Becke. Range-separated hybrid functionals[28,29] accurately predict a range of properties in (organic) main group chemistry.[30−39] Their formal properties suggest that they may also work well for transition metal complexes. To clarify this point, we review the performance of conventional semilocal and global hybrid functionals for transition metal chemistry.

Semilocal exchange-correlation functionals model the exchange-correlation energy density at a point **r** as a function of the electron density, density gradient, and possibly the noninteracting kinetic energy density and/or density Laplacian at **r**.[40,41] A key factor dictating their performance is their balance between self-interaction error and simulation of nondynamical (multireference) electron−electron correlation. Kohn−Sham DFT models the electron−electron interaction energy as the classical (Hartree) repulsion of the electron density plus an exchange-correlation correction. Self-interaction error refers to the fact

† Part of the "Walter Thiel Festschrift".

* To whom correspondence should be addressed. E-mail: guscus@rice.edu.

10.1021/jp902879m CCC: $40.75
Published on Web 07/08/2009

TABLE 1: Test Sets of Metal−Ligand Bond Lengths (MLBL) and Mean-Ligand Removal Enthalpies (MLRE) Used in This Paper[a]

label	test set
3d MLBL	$Sc(acac)_3$, $TiCl_4$, $TiMeCl_3$, $TiMe_2Cl_2$, $Ti(BD_4)_3$, VOF_3, VF_5, $VOCl_3$, $V(NMe_2)_4$, $VCp(CO)_4$, CrO_2F_2, CrO_2Cl_2, $CrO_2(NO_3)_2$, $Cr(\eta^6\text{-}C_6H_6)_2$, $Cr(\eta^6\text{-}C_6H_6)(CO)_3$, $Cr(NO)_4$, MnO_3F, $MnCp(CO_3)$, $Fe(CO)_5$, $Fe(CO)_3$(tmm), $Fe(CO)_2(NO)_2$, $FeCp_2$, $Fe(\eta^2\text{-}C_2H_4)(CO)_4$, $Fe(\eta^5\text{-}C_5Me_5)(\eta^5\text{-}P_5)$, $CoH(CO)_4$, $Co(CO)_3(NO)$, $Ni(CO)_4$, $Ni(acac)_2$ $Ni(PF_3)_4$, CuMe, CuCN, $Cu(acac)_2$
4d MLBL	$ZrCl_4$, $Zr(BH_4)_4$, $ZrCp_2Cl_2$, $NbCl_5$, $NbMe_2Cl_3$, $NbCp(\eta^7\text{-}C_7H_7)$, MoF_6, $MoOF_4$, $MoOCl_4$, MoO_2Cl_2, $Mo_2(OAc)_4$, $Mo(CO)_6$, RuO_4, $Ru(CO)_5$, $RuCp_2$, $Rh(NO)(PF_3)_3$, $RhCp(\eta^2\text{-}C_2H_4)_2$, CdMe, $CdMe_2$
5d MLBL	$HfCl_4$, $Hf(BH_4)_4$, $TaCl_5$, $TaMe_3F_2$, WF_6, WOF_4, $WSCl_4$, WMe_6, $W(CO)_6$, $WCp_2(H)_2$, Re_2F_8, $ReOCl_4$, ReO_3Me, $ReO_2Me(\eta^2\text{-}C_2H_2)$, OsO_4, $OsOCl_4$, $Os(CO)_5$, $Os(\eta^2\text{-}C_2H_4)(CO)_4$, IrF_6, $Pt(PF_3)_4$, Au(CO)Cl, $AuMe(PMe_3)$, HgMeCl, $Hg(CF_3)_2$, HgMe(CN)
3d hal MLBL	MnF_2, FeF_2, CoF_2, NiF_2, CuF, $MnCl_2$, $FeCl_2$, $CoCl_2$, $NiCl_2$, CuCl
3d MLRE	$TiBr_4$, $TiCp_2Cl_2$, $TiCl_4$, $TiOCl_2$, TiF_4, $TiOF_2$, TiO_2, $Cr(CO)_5$, $Cr(pyridine)(CO)_5$, $Cr(piperidine)(CO)_5$, $Cr(pyrazole)(CO)_5$, $Cr(CO)_6$, $Cr(\eta^6\text{-}C_6H_6)(CO)_3$, CrO_3, $Mn_2(CO)_{10}$, $Mn(COCH_3)(CO)_5$, $Cr(\eta^1\text{-}C_6H_5)(CO)_5$, $MnH(CO)_5$, $MnCl(CO)_5$, $Fe(CO)_4$, $Fe(\eta^2\text{-}C_2H_4)(CO)_4$, $Fe(CO)_5$, $FeH_2(CO)_4$, $FeCp_2$, $Co_2(CO)_8$, $CoH(CO)_4$, $Ni(CO)_4$, $Ni(CO)_3$, CuCl, CuF, $ZnEt_2$, $ZnMe_2$

[a] Here acac = acetylacetonato, Me = methyl, Cp = cyclopentadienyl, tmm = trimethylenemethane, Et = ethyl. The 3d MLBL and 3d hal MLBL sets were compiled in ref 19, and the 4d MLBL, 5d MLBL, and 3d MLRE sets were compiled in refs 21, 22, and 23, respectively.

that approximate exchange-correlation functionals may allow electrons to interact with themselves, such that, e.g., the total Hartree-exchange-correlation energy is nonzero in one-electron systems.[42] (A many-electron self-interaction error involving fractionally occupied (sub)systems has also been emphasized recently.[43−48]) Self-interaction error tends to overdelocalize electrons,[46] thus semilocal DFT systematically overestimates bond energies, underestimates bond lengths and barrier heights,[41] and underestimates the energies of Rydberg and charge-transfer excited states.[49] However, semilocal exchange functionals also have the benefit of mimicking nondynamical, left−right electron correlation in chemical bonds.[50−52]

Hybrid density functionals seek to balance these desirable vs undesirable effects of semilocal exchange by incorporating a fraction of one-electron self-interaction-free exact (Hartree−Fock-type, HF) exchange

$$E_x^{HF} = -\frac{1}{2}\sum_{ij}\int d^3\mathbf{r}_1 \int d^3\mathbf{r}_2 \frac{\psi_i^*(\mathbf{r}_1)\psi_j(\mathbf{r}_1)\psi_i(\mathbf{r}_2)\psi_j^*(\mathbf{r}_2)}{r_{12}} \quad (1)$$

Here $\{\psi_i(\mathbf{r})\}$ are the occupied orbitals of the noninteracting Kohn−Sham[53] reference system and $r_{12} \equiv |\mathbf{r}_1 - \mathbf{r}_2|$. Global hybrids such as the widely used B3LYP[54,55] incorporate a constant fraction of HF exchange. They have become the de facto approximations for much of (organic) main group computational chemistry, due to their remarkable combination of high accuracy and low computational cost. However, refs 18−23 suggest that the global hybrid approximation may be insufficiently flexible to accurately treat the broad range of binding situations (and amounts of nondynamical correlation) found in transition metal chemistry. Unlike in (organic) main group chemistry, global hybrids are at best slightly more accurate than their parent semilocal functionals for the transition metal sets of refs 18−23.

Range-separated hybrid functionals provide a more flexible admixture between HF and semilocal exchange, and thus show potential for treating the wide range of bonding motifs in transition metal chemistry. Range-separated hybrids split the Coulomb operator into short-range (SR) and long-range (LR) components, typically as

$$\frac{1}{r_{12}} = \underbrace{\frac{\mathrm{erfc}(\omega r_{12})}{r_{12}}}_{\mathrm{SR}} + \underbrace{\frac{\mathrm{erf}(\omega r_{12})}{r_{12}}}_{\mathrm{LR}}, \quad (2)$$

and use different fractions of HF exchange in each range. The parameter ω defines the separation between ranges, and is generally selected empirically. Perhaps the most widely used range-separated hybrids are long-range-corrected functionals combining short-range semilocal exchange with long-range HF exchange. Within this long-range-corrected hybrid approach, one may use explicit wave function-type approximations for long-range correlation, such as MP2,[56] CCSD,[57] CI,[29,58] MRCI,[59−61] or the random phase approximation (RPA);[62−64] another possibility is to combine range-separated exchange with a full range semilocal correlation functional.[33,37,65,66] These functionals are motivated by exact conditions: semilocal exchange accurately treats the electron−electron cusp,[67] while HF exchange provides the exact exchange-correlation functional in molecular density tails. Long-range-corrected hybrids such as LC-ωPBE[33,35] provide accurate treatments of thermochemistry and reaction barriers,[33,68] Raman activities,[39] charge-transfer excitation energies,[69,70] and other properties in (organic) main group chemistry and are thus highly promising for applications in homogeneous catalysis. Screened hybrids incorporate a fraction of short-range HF exchange.[31] They are designed to extend the accuracy of global hybrids to the solid state, where long-range HF exchange may be formally[71] and computationally[32] problematic. Their accurate predictions of kinetics[33] make them

promising for heterogeneous catalysis at metal surfaces. Finally, the observation that both screened and long-range-corrected hybrids can provide accurate main group thermochemical kinetics[33] led to recent "middle-range" hybrids that generalize eq 2 to multiple ranges.[36,38] The results of the present work validate our recent focus on range-separated hybrids, and illustrate their promise for transition metal chemistry.

Computational Details

We tested three range-separated hybrids developed in our research group: the HSE[31,34] short-range (screened) hybrid, the LC-ωPBE[33,35] long-range-corrected hybrid, and the HISS[36,38] middle-range hybrid. All three are constructed from the nonempirical Perdew−Burke−Ernzerhof (PBE)[72] generalized gradient approximation (GGA) semilocal functional and all of them use full range PBE correlation. To enable direct comparison with other approximations, we also report results for several semilocal and global hybrid functionals: LSDA (using the Vosko−Wilk−Nusair V correlation functional),[73] the BP86,[74,75] PBE,[72] and PBEsol[76] GGAs, the TPSS[77,78] and M06-L[79] meta-GGAs, and the B3LYP,[54,55] PBEh,[80,81] TPSSh,[82] and M06[83] global hybrids. Among these functionals, some of them are nonempirical[84] (LSDA, PBE, PBEsol, and TPSS) in their construction, others (including the range-separated hybrids) are minimally empirical in the sense that they contain only a few empirical parameters, and M06 and M06-L contain a large number of empirical parameters. Importantly for our purposes, both M06 and M06-L were parametrized to data sets containing transition metal compounds.[79,83]

Technical details of the calculations are as follows. All are self-consistent generalized Kohn−Sham[85,86] calculations in Gaussian basis sets, performed using a development version of the Gaussian[87] suite of programs. Most calculations were carried out using an "ultrafine" integration grid (a pruned version with 99 radial shells and 590 angular points per shell) to evaluate the semilocal exchange-correlation terms. M06 and M06-L seem to require larger grids,[39] so we used an unpruned grid with 200 radial shells and 974 angular points per shell for calculations using these two functionals. Open-shell systems were treated with the spin unrestricted formalism. Deviations are defined as "theory−experiment" or "theory−reference". "ME" and "MAE" denote mean and mean absolute errors.

Calculations on the geometric data sets of Bühl and co-workers[19,21,22] use the basis set BSI recommended by Martin and Sundermann,[88] incorporating the SDD basis set and effective core potential[89,90] augmented with 2f and 1g polarization functions on metals (contraction scheme [6s5p3d2f1g]) and the cc-pVTZ basis[91−93] on ligands. Notably, the 4d and 5d MLBL results reported here with BSI are very close to the quadruple-ζ results reported in refs 21 and 22. For the 3d MLBL set of ref 19, our results are in close agreement to those reported with the smaller svp and SDD (SDD without polarization functions on metals and 6-31G(d) on ligands) basis sets. Geometries were optimized in the symmetry recommended in refs 19, 21, and 22. (Exploratory calculations showed that some functionals had minima at lower symmetries, but this symmetry breaking had a negligible effect on the metal−ligand bond lengths in all tested cases.)

Calculations on the 3d MLRE of Johnson and Becke used the def2-qzvp all-electron basis set (contraction scheme [11s6p5d3f1g] on transition metals)[94] and TPSS/def2-tzvp[94] optimized geometries. Mean-ligand removal energies were obtained as the total fragmentation enthalpies of the transition metal complex into free transition metal atom(s) and neutral ligands, divided by the total number of metal−ligand and metal−metal bonds. Given that their structures could lead to some ambiguity, we clarify that we divide over a total of 11 bonds for $Mn_2(CO)_{10}$ and 9 bonds for $Co_2(CO)_8$.

Calculations on the 3d reaction energies of Furche and Perdew used TPSS/def2-qzvp optimized geometries, in order to separate the tested functionals' performance for geometric vs energetic properties. (We confirmed that LSDA/def2-qzvp and PBE/def2-qzvp calculations give nearly identical reaction energies at TPSS/def2-qzvp vs self-consistent geometries, such that our use of the former geometries should have little effect on the error statistics.) Our TPSS/def2-qzvp geometries are significantly different from the TPSS/qzvp geometries reported in ref 18 for V_2, $CoCl_3$, and Fe_2Cl_4.[95] All of our results use the lowest-energy solutions as described below. Note that Furche and Perdew gave results for MnH in the $^7\Sigma^+$ experimental ground state, even though they indicate that some methods predict a spurious $^5\Sigma^+$ ground state; we decided to give results with the predicted ground state for each functional. TPSS and all hybrid methods but B3LYP and M06 predict the ground state of MnH to be $^7\Sigma^+$; LC-ωPBE predicts a triplet as the ground state multiplicity of Sc_2 (all other methods predict the ground state to be a quintet). We have also recomputed the zero-point and thermal energy corrections to the dissociation energies of Fe_2Cl_4, $CoCl_3$, $Fe(CO)_5$, $Ni(CO)_4$, $Cr(C_6H_6)_2$, and $Fe(C_5H_5)_2$ in the test set of Furche and Perdew with the TPSS/def2-qzvp level of theory at self-consistent geometries. In addition, corrections due to scalar (Darwin and mass-velocity) relativistic effects to all reactions in this test set were recalculated using TPSS/def2-qzvp orbitals. Our reference energies are provided in Table 5.

The data sets of refs 19−22 contain vibrationally averaged bond lengths measured at finite temperature, which differ from the "vibrationless" classical-nuclei equilibrium bond lengths obtained from standard DFT calculations. Bühl et al. have reported zero-point corrections to these bond lengths in refs 20−22 These corrections were shown to be largely transferable between different functionals and basis sets for the 3d compounds, and to shift the mean errors by a nearly constant amount without reducing the error spread. For completeness, we report error statistics from zero-point corrected bond lengths as Supporting Information. These corrections do not qualitatively affect the conclusions below.

There have been multiple schemes proposed for determining the "correct" electronic state for DFT calculations on transition metal atoms and complexes. The present work follows Furche and Perdew and attempts to report results from the self-consistent broken-symmetry solution of lowest calculated energy.[18] We used stability analysis for most atoms and dimers to confirm that we had found the lowest energy state of each multiplicity. For atoms and dimers, we followed Furche and Perdew and calculated the ground state energies of all multiplicities predicted by BP86 to be $<10 - 20$ mH above the ground state, and selected the resulting minimum energy. For simplicity, we used the experimental multiplicities for the coordinatively saturated (and almost saturated) complexes in the test sets of Bühl and co-workers and Johnson and Becke. Note that the latter authors[23] used transition metal occupation schemes derived from current-density corrected DFT calculations,[96] based on the observation that current-dependent functionals can reduce the artificial level splitting of formally degenerate angular momentum eigenstates in atoms.[32,96] These authors also computed the MLRE of $Fe(CO)_4$ in the singlet state, while we used the experimental triplet state multiplicity.[97] For interested readers, we provide results of a natural population

TABLE 2: Mean and Mean Absolute Errors (in pm) in Predicted Equilibrium (r_e) Metal−Ligand Bond Lengths for Complexes from the MLBL Test Sets of Table 1 Relative to Experimentally Reported Values (r_a, r_α, or r_g)[a]

	3d hal MLBL		3d MLBL		4d MLBL		5d MLBL		Ave
functional	ME	MAE	ME	MAE	ME	MAE	ME	MAE	MAE[b]
TPSSh	−0.23	0.81	−1.49	1.66	−0.01	1.29	0.98	1.68	1.54
TPSS	−0.11	0.60	−0.81	1.31	0.75	1.48	1.71	2.15	1.65
PBE	−0.46	0.78	−0.92	1.63	0.64	1.38	1.55	1.98	1.66
M06-L	−0.95	1.03	−1.58	1.77	0.26	1.49	1.27	1.97	1.74
HSE	−0.33	0.75	−2.33	2.39	−0.88	1.48	0.11	1.37	1.75
PBEh	−0.28	0.82	−2.58	2.63	−1.24	1.62	−0.21	1.27	1.84
BP86	−0.55	0.83	−0.65	1.61	1.06	1.58	1.77	2.39	1.86
B3LYP	0.56	1.25	−0.45	1.79	1.22	1.85	1.90	2.24	1.96
PBEsol	−2.64	2.64	−2.90	2.96	−1.23	1.74	0.00	1.17	1.96
M06	−1.12	1.21	−1.83	2.01	0.26	1.82	1.07	2.21	2.01
HISS	−0.01	0.82	−3.02	3.05	−2.04	2.22	−1.07	1.47	2.25
LC-ωPBE	−1.11	1.15	−3.50	3.54	−2.59	2.65	−1.26	1.58	2.59
LSDA	−5.19	5.19	−4.56	4.56	−2.56	2.62	−1.16	1.50	2.89

[a] Geometry optimizations were performed with the BSI basis set. [b] "Ave MAE" denotes the average of the MAEs for the 3d, 4d, and 5d MLBL sets. Functionals are ordered from lowest to highest average MAE.

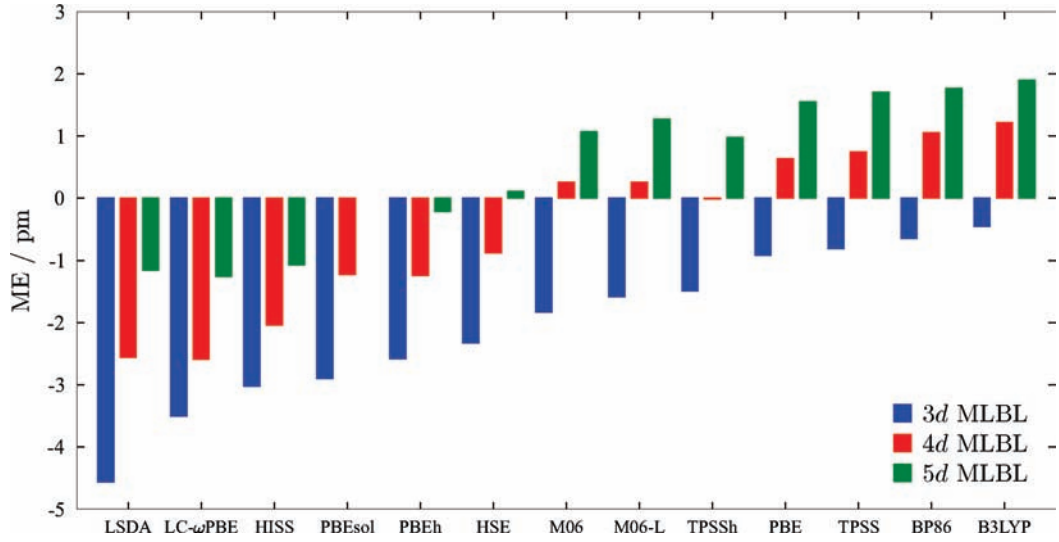

Figure 1. Mean errors for the 3d, 4d, and 5d MLBL test sets, details as in Table 2.

analysis on ground states of bare transition metal atoms as Supporting Information.

Results and Discussion

Geometries. Table 2 shows error statistics from the 3d, 4d, and 5d metal−ligand bond length (MLBL) sets of Bühl and co-workers. Negative (positive) mean errors correspond to too short (too long) bond lengths. For the 3d MLBL set, Bühl and Kabrede[19] observed that LSDA tends to overbind significantly, and that global hybrids do not provide a significant improvement over semilocal GGAs. Our results are consistent with these: LSDA overbinds, the BP86 and PBE GGAs correct most of this overbinding, and TPSS improves slightly on PBE results. The PBEh and TPSSh global hybrids show worse performance than the parent semilocal functional. The overbinding tendency of the PBE-based range-separated hybrids is discussed in more detail below. The M06 and M06-L functionals are close to the accurate TPSSh results. Overall, TPSS gives the lowest MAE.

For the 3d hal MLBL test set, all functionals but LSDA give reasonably low mean absolute erros. M06, LC-ωPBE, and M06-L tend to overbind, but LC-ωPBE overbinds considerably less than for the 3d MLBL test set. The lowest MAE is again given by TPSS. HISS shows very good results with a negligible mean error.

For the 4d MLBL test set, ref 21 shows that all methods but LSDA tend to underbind and hybrid methods tend to outperform their parent semilocal density functionals. Our results show that LSDA, PBEh, and the PBE-based range-separated hybrids all tend to overbind. Although TPSSh does perform better than TPSS, PBE and M06-L yield lower mean absolute errors than the PBEh and M06 hybrids. TPSSh gives the best performance on this test set considering the low MAE and an almost 0 mean error.

Reference 22 showed that, surprisingly, LSDA outperforms all other functionals for the 5d MLBL test set. Reference 22 also demonstrated that calculations with relativistic effective core potentials yield results very close to all-electron scalar relativistic calculations. (This validates our focus on ECP calculations.) Table 2 shows that LSDA, PBEh, and all range-separated hybrids provide a very good performance for this test set. While hybrids tend to outperform the parent semilocal functional, we do not think this is a general trend (see below).

The differences between the 3d, 4d, and 5d MLBL test sets are best illustrated by Figure 1, which summarizes the mean errors for each functional. The mean errors show a systematic trend: all functionals overbind less (or underbind more) when moving down the periodic table from 3d to 5d metals. The slope of this trend, or the difference between 3d and 5d mean errors,

TABLE 3: Deviations (in pm) in Predicted Equilibrium (r_e) Bond Lengths Relative to Experimental Measurements for the M−Cl Distance in $TiCl_4$, $ZrCl_4$, and $HfCl_4$, and the Mean M−C Distance in $Fe(CO)_5$, $Ru(CO)_5$, and $Os(CO)_5$[a]

complex	HF	LC-ωPBE	TPSS	B3LYP
$TiCl_4$	−0.05	−2.70	0.63	0.44
$ZrCl_4$	1.45	−1.82	0.70	0.83
$HfCl_4$	3.01	−0.22	1.93	2.16
$Fe(CO)_5$	11.97	−4.07	−2.25	−1.28
$Ru(CO)_5$	4.61	−2.63	−1.10	−0.39
$Os(CO)_5$	3.71	−1.02	0.47	0.98

[a] Calculations use the BSI basis set.

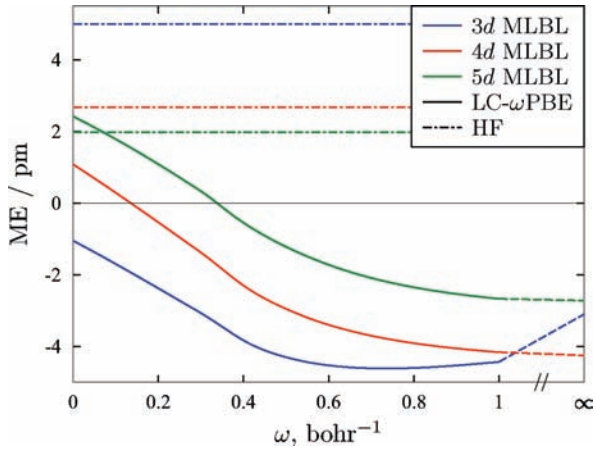

Figure 2. Mean errors for the 3d, 4d, and 5d MLBL test sets, calculated using the LC-ωPBE long-range-corrected hybrid functional form and plotted as a function of ω. Calculations use the def2-svp basis set. ω = ∞ corresponds to HF exchange and PBE correlation. HF results are also given as a reference.

is fairly constant around 2.5 pm. The HISS multiple-range hybrid has a relatively small slope in the mean errors, suggesting a smaller systematic error. Comparison with previous results[19] suggests that the trend will still hold with larger (qzvp) basis sets, and the relative difference between the 3d and 5d test sets will decrease slightly. We note that, while higher-order relativistic effects may play a role in this trend, ref 22 showed that ECP calculations on these complexes yield results very close to all-electron scalar relativistic calculations.

We tested whether this trend is an artifact of the different test sets' composition (see Table 1) by examining two homologous sets of complexes: the M−Cl distance in $TiCl_4$, $ZrCl_4$, and $HfCl_4$, and the mean M−C distance in $Fe(CO)_5$, $Ru(CO)_5$, and $Os(CO)_5$. Table 3 reports results from representative methods. The trend of Figure 1 still holds for semilocal and hybrid functionals. Hartree−Fock theory shows an interesting behavior: the metal−halide bond tends to more underbinding as one goes down in the periodic table with the metal, but the reverse is observed for the metal−carbonyl bond length. In particular, the Hartree−Fock M−C distance in $Fe(CO)_5$ is tremendously erroneous. It seems that the reversed order observed for HF when considering the entire sets (see for instance Figure 2) is due to the very large underbinding for some molecules in the 3d set, a condition that is somehow alleviated for heavier transition metals.

The results in Table 2 indicate that all of the PBE hybrids (PBEh, HSE, HISS, and LC-ωPBE) overbind more than either PBE or Hartree−Fock theory (in Figure 2). This appears to be in part a mismatch between HF exchange and the PBE correlation functional. To illustrate, we computed the mean errors for the *x*d MLBL series using the LC-ωPBE functional form (short-range PBE exchange, long-range HF exchange, full range PBE correlation) with different values of ω. These calculations used the def2-svp[94] basis set. Results are shown in Figure 2. The functional significantly overbinds in the $\omega \rightarrow \infty$ limit of Hartree−Fock exchange and PBE correlation. The least negative mean errors are obtained at the $\omega = 0$ limit of the PBE hole model, which is very close to PBE.[98] The ω yielding zero mean error is zero for the 3d series, very small for the 4d series, and close to the published LC-ωPBE 0.4 $bohr^{-1}$ for the 5d series. Thus, our existing PBE-based long-range hybrids cannot improve upon PBE for the 3d and 4d bond lengths. However, further improvements in semilocal correlation functionals, and range separation of semilocal correlation, might well yield improved results.

TABLE 4: Mean and Mean Absolute Errors (in kcal mol^{-1}) in Predicted Mean-Ligand Removal Energies of Complexes in the 3d MLRE Test Set of Table 1[a]

functional	ME	MAE	max	
LC-ωPBE	−1.0	2.5	−14.7	CrO_3
PBEh	−1.9	2.5	−17.1	CrO_3
HSE	−2.0	2.6	−16.9	CrO_3
M06	−1.5	3.3	−11.7	$FeCp_2$
TPSSh	2.7	3.8	7.9	$MnH(CO)_5$
B3LYP	−4.3	4.4	−20.3	$FeCp_2$
M06-L	4.8	5.3	12.2	$TiOCl_2$
HISS	−5.6	5.6	−30.8	CrO_3
TPSS	7.1	7.5	12.5	$MnH(CO)_5$
BP86	8.2	8.7	17.6	TiO_2
PBE	9.4	9.5	17.7	TiO_2
PBEsol	16.6	16.6	27.3	TiO_2
LSDA	26.0	26.0	44.3	TiO_2

[a] Calculations use the def2-qzvp basis and TPSS/def2-tzvp geometries.

In order to compare the accuracy in the prediction of bond lengths of coordinatively saturated transition metal complexes with that of main group compounds, we have assessed the performance of all density functionals in the test set of ref 99. These results are included as an appendix.

Energetics. Table 4 shows error statistics for the 3d MLRE set of Johnson and Becke.[23] All of the functionals save LSDA and PBEsol are reasonably accurate, and hybrid functionals outperform the corresponding semilocal functionals. The long-range-corrected LC-ωPBE hybrid is especially accurate, with a small mean error. The highly parametrized M06-L meta-GGA, while outperforming other semilocal functionals, is still inferior to all hybrid functionals considered but HISS. The fact that most methods show their largest error for transition metal oxides (TiO_2, CrO_3) is consistent with the observation by Riley and Merz[24] that density functionals give large errors in predicting the enthalpies of formation of oxides and complexes with chromium.

Table 5 shows the predicted reaction energies for the test set of Furche and Perdew.[18] Our results largely agree with those of ref 18. The M06 functionals yield very low mean absolute errors, consistent with ref 83 and with their being parametrized to a data set similar to this one.[79,83] While the overall errors for hybrid functionals are somewhat larger than for GGAs, inspection of Table 5 shows that the hybrid errors are largest for bare metal dimers. We expect that the poor results for bare metal dimers point to a fundamental limitation of range-separated hybrids incorporating a universal range separation parameter ω (eq 2). This is analogous to HSE's limitations for simple bulk metals pointed out in ref 100. In addition, admixture of long-

TABLE 5: Predicted Reaction Energies for Each System in the Reference Test Set of Furche and Perdew[a]

	ref.	LSDA	BP86	PBE	TPSS	B3LYP	PBEh	TPSSh	HSE	LC-ωPBE	HISS	M06	M06-L	PBEsol
$Sc_2 \rightarrow 2Sc$	39.7	54.7	35.9	38.6	32.4	11.8	17.6	24.6	18.0	8.4	6.9	22.3	31.1	46.3
$V_2 \rightarrow 2V$	62.1	112.3	80.0	76.4	67.2	31.6	10.0	41.1	10.9	1.0	−12.8	48.4	60.9	87.5
$Ni_2 \rightarrow 2Ni$	46.4	82.3	61.8	62.9	58.7	37.6	36.2	43.9	36.7	33.3	31.3	44.8	45.4	70.0
$CrH \rightarrow Cr + H$	45.7	60.3	56.7	52.4	57.4	54.9	48.7	55.9	48.5	51.2	46.5	51.4	58.4	54.3
$MnH \rightarrow Mn + H$	32.0	56.2	52.0	48.1	52.2	42.0	43.6	50.9	43.6	50.7	45.0	38.4	40.5	50.4
$CoH \rightarrow Co + H$	46.8	72.9	64.4	61.7	64.3	61.6	57.6	62.9	57.4	58.1	54.5	61.3	58.8	65.0
$TiO \rightarrow Ti + O$	158.9	210.0	183.5	183.1	173.9	160.5	160.1	165.5	159.7	162.0	149.0	155.2	162.6	192.6
$MnO \rightarrow Mn + O$	90.8	149.8	127.3	127.5	120.1	94.7	93.9	106.5	94.1	103.3	86.2	78.8	94.6	136.7
$CuO \rightarrow Cu + O$	63.9	95.3	77.1	77.7	73.0	63.6	61.8	66.8	61.5	67.2	58.9	61.3	71.0	83.8
$ScF \rightarrow Sc + F$	143.0	175.9	154.7	155.6	151.4	143.4	142.2	146.5	142.4	146.6	138.5	146.9	150.7	163.2
$CrF \rightarrow Cr + F$	105.2	136.7	119.4	119.1	117.8	114.1	109.1	113.9	108.9	116.9	108.7	111.5	116.5	124.7
$CuF \rightarrow Cu + F$	102.5	119.9	100.4	101.5	99.4	93.4	92.5	95.9	92.0	101.1	93.7	92.8	98.1	107.9
$Fe_2Cl_4 \rightarrow 2FeCl_2$	35.2	51.6	33.1	34.9	32.5	26.4	30.3	30.4	30.4	29.6	29.2	40.2	34.3	41.7
$CoCl_3 \rightarrow CoCl_2 + 1/2Cl_2$	16.0	42.5	28.5	29.3	26.2	28.0	27.0	36.8	27.8	17.8	17.0	22.1	33.0	33.1
$Fe(CO)_5 \rightarrow Fe(CO)_4 + CO$	41.7	62.6	45.4	47.5	46.6	37.6	45.2	45.7	44.8	46.3	43.6	40.1	44.8	55.5
$Ni(CO)_4 \rightarrow Ni(CO)_3 + CO$	24.3	42.4	27.8	29.4	28.9	19.6	24.7	26.9	24.8	26.0	23.8	21.3	26.7	36.1
$1/2Cr(C_6H_6)_2 \rightarrow 1/2Cr + C_6H_6$	31.4	64.4	35.0	37.4	38.7	13.6	21.5	32.1	21.1	27.7	15.5	26.2	37.9	50.7
$1/2Fe(C_5H_5)_2 \rightarrow 1/2Fe + C_5H_5$	79.9	127.7	92.9	96.5	94.7	67.9	78.3	87.9	77.8	90.3	76.4	76.6	91.0	112.0
ME		30.7	11.7	11.9	9.4	−3.5	−3.6	3.8	−3.6	−1.6	−8.5	−1.4	5.0	19.2
MAE		30.7	12.6	12.2	10.9	10.3	9.0	9.4	9.0	11.4	11.6	6.8	6.8	19.2
ME*		30.1	12.1	12.3	10.7	0.3	1.3	7.2	1.2	5.2	−2.1	0.5	6.8	19.4
MAE*		30.1	12.6	12.5	11.4	7.8	5.2	8.7	5.3	6.6	5.8	5.9	7.5	19.4

[a] Calculations use the def2-qzvp basis and TPSS/def2- qzvp opitmized geometries. ME and MAE denote mean and mean absolute errors for the entire test set. ME* and MAE* denote errors leaving out Sc_2, V_2, and Ni_2 (see text). Reference values were corrected from those in ref 18 as described in Computational Details.

range exact exchange with long-range semilocal correlation might be inadequate for systems with significant nondynamical correlation (as is the case of transition metal dimers). Long-range-corrected hybrids with explicit wave function-type long-range correlation[29,56−64] could alleviate this problem although at a considerably larger computational cost.

Table 5 also shows statistical errors leaving out bare metal dimers. Statistical results for these "typical" systems are in line with those of Table 4, and indicate that range separated hybrids are quite accurate for these systems. Indeed, HSE and PBEh are the best performers for this modified Furche and Perdew reference set, with LC-ωPBE, HISS, and M06 also providing reasonable results. The mean absolute errors are also closer to those seen for (organic) main group chemistry.[35] Comparison of Tables 4 and 5 suggests that M06 and M06-L, which were parametrized to data sets including transition metal dimers, may have sacrificed accuracy for "typical" systems in favor of accuracy for bare metal dimers.

Conclusions

We have reported an assessment of the ability of different density functionals, with emphasis on range- separated hybrids, to predict metal−ligand bond lengths and reaction energies. Our results indicate that range-separated hybrids show a great deal of promise for these systems. They also point to the importance of range-separated correlation in improving these functionals. The metal−ligand bond lengths of our PBE- based range-separated hybrids appear to be degraded by a mismatch between HF exchange and semilocal PBE correlation.

An important extension of this work will be whether the LC-ωPBE's accurate prediction of main group reaction barriers[35] will carry over to transition metal chemistry. This will require test sets of accurate barrier heights of transition metal reactions, which we regard as a principle desideratum of the field. Applications of screened and middle-range hybrids to reactions at metal surfaces should also prove instructive.

Acknowledgment. This work was supported by the National Science Foundation (CHE-0807194) and the Welch Foundation (C-0036). We thank Axel D. Becke and Erin R. Johnson for an advance copy of ref 23. C.A.J.H. also thanks Yan Zhao for helpful discussions on the implementation of the M06 functionals.

TABLE 6: Mean and Mean Absolute Errors (in pm) in Predicted Equilibrium Bond Lengths of the 19 Main Group Compounds from Ref 99[a]

	ab initio		empirical	
functional	ME	MAE	ME	MAE
M06-L	−0.02	0.41	−0.06	0.41
TPSSh	0.20	0.49	0.16	0.44
B3LYP	−0.09	0.48	−0.13	0.47
TPSS	0.77	0.79	0.73	0.74
HSE	−0.43	0.74	−0.47	0.77
PBEh	−0.43	0.77	−0.47	0.80
M06	−0.54	0.86	−0.58	0.89
LC-ωPBE	−0.68	0.91	−0.72	0.95
PBE	1.01	1.01	0.97	0.97
BP86	1.10	1.10	1.06	1.06
PBEsol	0.92	1.11	0.88	1.12
LSDA	0.53	1.29	0.48	1.30
HISS	−1.33	1.33	−1.37	1.37

[a] The errors are shown against high level ab initio (CCSD(T)/cc-pCVQZ) calculations from Ref 99 and against empirical reference values provided in the same reference. Calculations use the cc-pVTZ basis set.

Appendix

Table 6 shows error statistics of the performance of all density functional approximations considered in the prediction of the equilibrium bond lengths of the 19 main group compounds of ref 99 using the cc-pVTZ basis set. Two different reference values are considered, namely high level ab initio calculations (CCSD(T)/cc-pCVQZ) and the empirically corrected experimental values as given in ref 99. Only BP86, PBEsol, LSDA, and HISS give mean absolute errors larger than 1 pm when compared to the empirical values. The mean absolute errors could be directly compared to the average mean absolute error of Table 2, which shows that M06, HISS, LC-ωPBE, and LSDA

give errors larger than 2 pm. The average bond length in the test set of ref 99 is 111.94 pm, so that the error of TPSSh for the bond lengths in this set is approximately 0.4%. On the other hand, the average of the average bond length of the 3d, 4d, and 5d MLBL test sets is 201.31 pm, so that the error of TPSSh for bond lengths in coordinatively saturated (or almost saturated) complexes is approximately 0.8%. One has to remember, though, that the bond lengths from ref 99 are truly equilibrium bond lengths, whereas the experimental values for the bond lengths in the transition metal complexes have not been corrected for zero-point and thermal effects. It is still noteworthy that the best functionals predict bond lengths of transition metal complexes to within 1% of the experimental value, and this accuracy is comparable to that achieved for main group compounds.

Supporting Information Available: Natural population analysis of the lowest-energy, self-consistent, broken-symmetry solution for bare transition metal atoms, equilibrium bond lengths for systems in the 3d, 4d, 5d, and 3d hal MLBL test sets (including statistics with zero-point-corrected bond lengths), and mean ligand removal enthalpies of complexes in the 3d MLRE test set. This material is available free of charge via the Internet at http://pubs.acs.org.

References and Notes

(1) Jonas, V.; Thiel, W. *J. Chem. Phys.* **1995**, *102*, 8474.

(2) Méndez, M.; Paz Muñoz, M.; Nevado, C.; Cárdenas, D. J.; Echevarren, A. M. *J. Am. Chem. Soc.* **2001**, *123*, 10511.

(3) Reetz, M. T.; Meiswinkel, A.; Mehler, G.; Angermund, K.; Graf, M.; Thiel, W.; Mynott, R.; Blackmond, D. G. *J. Am. Chem. Soc.* **2005**, *127*, 10305.

(4) Shaik, S.; Kumar, D.; de Visser, S. P.; Altun, A.; Thiel, W. *Chem. Rev.* **2005**, *105*, 2279.

(5) *Computational Transition Metal Chemistry*; Davidson, E., Ed.; American Chemical Society: Washington, DC, 2000; Vol. *100*.

(6) Scuseria, G. E.; Schaefer, H. F., III *Chem. Phys. Lett.* **1990**, *174*, 501.

(7) Thiel, W.; Voityuk, A. A. *J. Phys. Chem.* **1996**, *100*, 616.

(8) Bartlett, R. J.; Schweigert, I. V.; Lotrich, V. F. *J. Mol. Struct. (THEOCHEM)* **2006**, *771*, 1.

(9) Curtiss, L. A.; Redfern, P. C.; Raghavachari, K. *J. Chem. Phys.* **2005**, *123*, 124107.

(10) Zhao, Y.; Lynch, B. J.; Truhlar, D. G. *Phys. Chem. Chem. Phys.* **2005**, *7*, 43.

(11) Chakravorty, S. J.; Gwaltney, S. R.; Davidson, E. R.; Parpia, F. A.; Fischer, C. F. *Phys. Rev. A* **1993**, *47*, 3649.

(12) Baerends, E. J.; Ros, P. *Mol. Phys.* **1975**, *30*, 1735.

(13) Ziegler, T. *Can. J. Chem.* **1995**, *73*, 743.

(14) Li, J.; Schreckenbach, G.; Ziegler, T. *J. Am. Chem. Soc.* **1995**, *117*, 486.

(15) Bérces, A.; Ziegler, T. In *Topics in Current Chemistry*; Nalewajski, R. F., Ed.; Springer: Berlin, 1996; Vol. *182*, pp 41−85.

(16) Görling, A.; Trickey, S. B.; Gisdakis, P.; Rösch, N. In *Topics in Organometallic Chemistry*; Brown, J. M., Hofmann, P., Eds.; Springer: Berlin, 1999; Vol. 4, pp 109−163.

(17) Harvey, J. N. *Annu. Rep. Prog. Chem., Sect. C* **2006**, *102*, 203.

(18) Furche, F.; Perdew, J. P. *J. Chem. Phys.* **2006**, *124*, 044103.

(19) Bühl, M.; Kabrede, H. *J. Chem. Theory Comput.* **2006**, *2*, 1282.

(20) Waller, M. P.; Bühl, M. *J. Comput. Chem.* **2006**, *28*, 1531.

(21) Waller, M. P.; Braun, H.; Hojdis, N.; Bühl, M. *J. Chem. Theory Comput.* **2007**, *3*, 2234.

(22) Bühl, M.; Reimann, C.; Pantazis, D. A.; Bredow, T.; Neese, F. *J. Chem. Theory Comput.* **2008**, *4*, 1449.

(23) Johnson, E. R.; Becke, A. D. *Can. J. Chem.*, accepted for publication.

(24) Riley, K. E.; Merz, K. M., Jr. *J. Phys. Chem. A* **2007**, *111*, 6044.

(25) Schultz, N. E.; Zhao, Y.; Truhlar, D. G. *J. Phys. Chem. A* **2005**, *109*, 11127.

(26) Schultz, N. E.; Zhao, Y.; Truhlar, D. G. *J. Phys. Chem. A* **2005**, *109*, 4388.

(27) Hyla-Krispin, I.; Grimme, S. *Organometallics* **2004**, *23*, 5581.

(28) Savin, A. In *Recent Developments and Applications of Modern Density Functional Theory*; Seminario, J. M., Ed.; Elsevier: Amsterdam, 1996; pp 327−357.

(29) Leininger, T.; Stoll, H.; Werner, H.-J.; Savin, A. *Chem. Phys. Lett.* **1997**, *275*, 151.

(30) Iikura, H.; Tsuneda, T.; Yanai, T.; Hirao, K. *J. Chem. Phys.* **2001**, *115*, 3540.

(31) Heyd, J.; Scuseria, G. E.; Ernzerhof, M. *J. Chem. Phys.* **2003**, *118*, 8207; **2006**, *124*, 219906(E).

(32) Heyd, J.; Scuseria, G. E. *J. Chem. Phys.* **2004**, *121*, 1187.

(33) Vydrov, O. A.; Heyd, J.; Krukau, A. V.; Scuseria, G. E. *J. Chem. Phys.* **2006**, *125*, 074106.

(34) Krukau, A. V.; Vydrov, O. A.; Izmaylov, A. F.; Scuseria, G. E. *J. Chem. Phys.* **2006**, *125*, 224106.

(35) Vydrov, O. A.; Scuseria, G. E. *J. Chem. Phys.* **2006**, *125*, 234109.

(36) Henderson, T. M.; Izmaylov, A. F.; Scuseria, G. E.; Savin, A. *J. Chem. Phys.* **2007**, *127*, 221103.

(37) Cohen, A. J.; Mori-Sánchez, P.; Yang, W. *J. Chem. Phys.* **2007**, *126*, 191109.

(38) Henderson, T. M.; Izmaylov, A. F.; Scuseria, G. E.; Savin, A. *J. Chem. Theory Comput.* **2008**, *4*, 1254.

(39) Jiménez-Hoyos, C. A.; Janesko, B. G.; Scuseria, G. E. *Phys. Chem. Chem. Phys.* **2008**, *10*, 6621.

(40) Perdew, J. P.; Schmidt, K. In *Density Functional Theory and its Application to Materials*; Van Doren, V., Van Alsenoy, C., Geerlings, P., Eds.; American Institute of Physics: Melville, NY, 2001; pp 1−20.

(41) Scuseria, G. E.; Staroverov, V. N. In *Theory and Applications of Computational Chemistry: The First 40 Years*; Dykstra, C. E., Frenking, G., Kim, K. S., Scuseria, G. E., Eds.; Elsevier: Amsterdam, 2005; pp 669−724.

(42) Perdew, J. P.; Zunger, A. *Phys. Rev. B* **1981**, *23*, 5048.

(43) Vydrov, O. A.; Scuseria, G. E.; Perdew, J. P. *J. Chem. Phys.* **2007**, *126*, 154109.

(44) Perdew, J. P.; Ruzsinszky, A.; Csonka, G. I.; Vydrov, O. A.; Scuseria, G. E.; Staroverov, V. N.; Tao, J. *Phys. Rev. A* **2007**, *76*, 040501.

(45) Ruzsinszky, A.; Perdew, J. P.; Csonka, G. I.; Vydrov, O. A.; Scuseria, G. E. *J. Chem. Phys.* **2007**, *126*, 104102.

(46) Cohen, A. J.; Mori-Sánchez, P.; Yang, W. *Phys. Rev. B* **2008**, *77*, 115123.

(47) Mori-Sánchez, P.; Cohen, A. J.; Yang, W. *Phys. Rev. Lett.* **2008**, *100*, 146401.

(48) Cohen, A. J.; Mori-Sánchez, P.; Yang, W. *Science* **2008**, *321*, 792.

(49) Dreuw, A.; Weisman, J. L.; Head-Gordon, M. *J. Chem. Phys.* **2003**, *119*, 2943.

(50) Gritsenko, O. V.; Schipper, P. R. T.; Baerends, E. J. *J. Chem. Phys.* **1997**, *107*, 5007.

(51) Cremer, D. *Mol. Phys.* **2001**, *99*, 1899.

(52) Baerends, E. J.; Gritsenko, O. V. *J. Chem. Phys.* **2005**, *123*, 062202.

(53) The hybrid calculations performed in this work treat a generalized Kohn−Sham reference system with a nonlocal exchange-correlation potential, following refs 85 and 86.

(54) Becke, A. D. *J. Chem. Phys.* **1993**, *98*, 5648.

(55) Lee, C.; Yang, W.; Parr, R. G. *Phys. Rev. B* **1988**, *37*, 785.

(56) Ángyán, J. G.; Gerber, I. C.; Savin, A.; Toulouse, J. *Phys. Rev. A* **2005**, *72*, 012510.

(57) Goll, E.; Werner, H.-J.; Stoll, H. *Phys. Chem. Chem. Phys.* **2005**, *7*, 3917.

(58) Pollet, R.; Savin, A.; Leininger, T.; Stoll, H. *J. Chem. Phys.* **2002**, *116*, 1250.

(59) Toulouse, J.; Colonna, F.; Savin, A. *Phys. Rev. A* **2004**, *70*, 062505.

(60) Toulouse, J.; Colonna, F.; Savin, A. *J. Chem. Phys.* **2005**, *122*, 014110.

(61) Fromager, E.; Jensen, H. J. A. *Phys. Rev. A* **2008**, *78*, 022504.

(62) Scuseria, G. E.; Henderson, T. M.; Sorensen, D. C. *J. Chem. Phys.* **2008**, *129*, 231101.

(63) Janesko, B. G.; Henderson, T. M.; Scuseria, G. E. *J. Chem. Phys.* **2009**, *130*, 081105.

(64) Toulouse, J.; Gerber, I. C.; Jansen, G.; Savin, A.; Ángyán, J. G. *Phys. Rev. Lett.* **2009**, *102*, 096404.

(65) Gerber, I. C.; Ángyán, J. G. *Chem. Phys. Lett.* **2005**, *415*, 100.

(66) Chai, J.-D.; Head-Gordon, M. *J. Chem. Phys.* **2008**, *128*, 084106.

(67) Burke, K.; Perdew, J. P.; Ernzerhof, M. *J. Phys. Chem.B* **1998**, *109*, 3760.

(68) Song, J.-W.; Hirosawa, T.; Tsuneda, T.; Hirao, K. *J. Chem. Phys.* **2007**, *126*, 154105.

(69) Lange, A. W.; Rohrdanz, M. A.; Herbert, J. M. *J. Phys. Chem. B* **2008**, *112*, 6304.

(70) Rohrdanz, M. A.; Martins, K. M.; Herbert, J. M. *J. Chem. Phys.* **2009**, *130*, 054112.

(71) Monkhorst, H. J. *Phys. Rev. B* **1979**, *20*, 1504.

(72) Perdew, J. P.; Burke, K.; Ernzerhof, M. *Phys. Rev. B* **1986**, *33*, 8822; **1986**, *34*, 7406(E).

(73) Vosko, S. H.; Wilk, L.; Nusair, M. *Can. J. Phys.* **1980**, *58*, 1200.

(74) Becke, A. D. *Phys. Rev. A* **1988**, *38*, 3098.
(75) Perdew, J. P. *Phys. Rev. B* **1988**, *37*, 785.
(76) Perdew, J. P.; Ruzsinszky, A.; Csonka, G. I.; Vydrov, O. A.; Scuseria, G. E.; Constantin, L. A.; Zhou, X.; Burke, K. *Phys. Rev. Lett.* **2008**, *100*, 136406; **2009**, *102*, 039902(E).
(77) Tao, J.; Perdew, J. P.; Staroverov, V. N.; Scuseria, G. E. *Phys. Rev. Lett.* **2003**, *91*, 146401.
(78) Perdew, J. P.; Tao, J.; Staroverov, V. N.; Scuseria, G. E. *J. Chem. Phys.* **2004**, *120*, 6898.
(79) Zhao, Y.; Truhlar, D. G. *J. Chem. Phys.* **2006**, *125*, 194101.
(80) Adamo, C.; Barone, V. *J. Chem. Phys.* **1999**, *110*, 6158.
(81) Ernzerhof, M.; Scuseria, G. E. *J. Chem. Phys.* **1999**, *110*, 5029.
(82) Staroverov, V. N.; Scuseria, G. E.; Tao, J.; Perdew, J. P. *J. Chem. Phys.* **2003**, *119*, 12129; **2004**, *121*, 11507(E).
(83) Zhao, Y.; Truhlar, D. G. *Theor. Chem. Acc.* **2008**, *120*, 215.
(84) Perdew, J. P.; Ruzsinszky, A.; Tao, J.; Staroverov, V. N.; Scuseria, G. E.; Csonka, G. I. *J. Chem. Phys.* **2005**, *123*, 062201.
(85) Seidl, A.; Görling, A.; Vogl, P.; Majewski, J. A.; Levy, M. *Phys. Rev. B* **1996**, *53*, 3764.
(86) Neumann, R.; Nobes, R. H.; Handy, N. C. *Mol. Phys.* **1996**, *87*, 1.
(87) Frisch, M. J.; et al. *Gaussian Development Version*, revision G.01; Gaussian, Inc.: Wallingford, CT, 2007.
(88) Martin, J. M. L.; Sundermann, A. *J. Chem. Phys.* **2001**, *114*, 3408.
(89) Dolg, M.; Weidig, U.; Stoll, H.; Preuss, H. *J. Chem. Phys.* **1987**, *86*, 866.
(90) Andrae, D.; Häussermann, U.; Dolg, M.; Stoll, H.; Preuss, H. *Theor. Chem. Acc.* **1990**, *77*, 123.
(91) Dunning, T. H., Jr. *J. Chem. Phys.* **1989**, *90*, 1007.
(92) Woon, D. E.; Dunning, T. H., Jr. *J. Chem. Phys.* **1993**, *98*, 1358.
(93) Wilson, A. K.; Woon, D. E.; Peterson, K. A.; Dunning, T. H., Jr. *J. Chem. Phys.* **1999**, *110*, 7667.
(94) Weigend, F.; Ahlrichs, R. *Phys. Chem. Chem. Phys.* **2005**, *7*, 3297.
(95) Furche, F.; Perdew, J. P. *J. Chem. Phys.,* erratum to ref 18 in preparation.
(96) Johnson, E. R.; Dickson, R. M.; Becke, A. D. *J. Chem. Phys.* **2007**, *126*, 184104.
(97) Note that $Fe(CO)_4$ also appears in the test set of Furche and Perdew. In that case, we used the singlet state since the dissociation of CO from $Fe(CO)_5$ is believed to yield singlet $Fe(CO)_4$.
(98) Ernzerhof, M.; Perdew, J. P. *J. Phys. Chem.* **1998**, *109*, 3313.
(99) Bak, K. L.; Gauss, J.; Jørgensen, P.; Olsen, J.; Helgaker, T.; Stanton, J. F. *J. Chem. Phys.* **2001**, *114*, 6548.
(100) Paier, J.; Marsman, M.; Hummer, K.; Kresse, G.; Gerber, I. C.; Ángyán, J. G. *J. Chem. Phys.* **2006**, *124*, 154709; **2006**, *125*, 249901(E).

JP902879M